The mitochondrial fission receptor Mff selectively recruits oligomerized Drp1

Raymond Liu and David C. Chan
Division of Biology and Biological Engineering, California Institute of Technology, Pasadena, CA 91125

ABSTRACT **Dynamin-related protein 1 (Drp1) is the GTP-hydrolyzing mechanoenzyme that catalyzes mitochondrial fission in the cell. Residing in the cytosol as dimers and tetramers, Drp1 is recruited by receptors on the mitochondrial outer membrane, where it further assembles into a helical ring that drives division via GTP-dependent constriction. The Drp1 receptor Mff is a major regulator of mitochondrial fission, and its overexpression results in increased fission. In contrast, the alternative Drp1 receptors MiD51 and MiD49 appear to recruit inactive forms of Drp1, because their overexpression inhibits fission. Using genetic and biochemical assays, we studied the interaction of Drp1 with Mff. We show that the insert B region of Drp1 inhibits Mff–Drp1 interactions, such that recombinant Drp1 mutants lacking insert B form a stable complex with Mff. Mff cannot bind to assembly-deficient mutants of Drp1, suggesting that Mff selectively interacts with higher-order complexes of Drp1. In contrast, the alternative Drp1 receptors MiD51 and MiD49 can recruit Drp1 dimers. Therefore Drp1 recruitment by Mff versus MiD51 and MiD49 may result in different outcomes because they recruit different subpopulations of Drp1 from the cytosol.**

Monitoring Editor
Donald D. Newmeyer
La Jolla Institute for Allergy and Immunology

Received: Aug 21, 2015
Revised: Sep 29, 2015
Accepted: Sep 30, 2015

INTRODUCTION

Mitochondria are dynamic organelles that continuously undergo regulated cycles of fission and fusion. These processes are essential for maintaining mitochondrial health and function and have important roles in mitochondrial DNA stability and inheritance, respiratory capacity, apoptosis, and mitophagy (Westermann, 2010; Chan, 2012; Youle and van der Bliek, 2012). Fission is mediated by dynamin-related protein 1 (Drp1), a member of the dynamin superfamily of GTPases (Smirnova *et al.*, 2001). Like dynamin, Drp1 is a mechanoenzyme that has the capacity to self-assemble into oligomeric complexes that have enhanced GTP hydrolysis activity (Ferguson and De Camilli, 2012). In the cell, much of Drp1 resides in the cytosol, but it can be recruited to mitochondria via receptors anchored to the mitochondrial outer membrane (Loson *et al.*, 2013). Once recruited, Drp1 further assembles around the mitochondrial tubule to form an oligomeric ring that constricts and divides the mitochondrion in a GTP-dependent process (Ingerman *et al.*, 2005; Mears *et al.*, 2011). Mutation of Drp1 blocks mitochondrial fission, resulting in elongated mitochondrial networks due to unopposed mitochondrial fusion (Smirnova *et al.*, 2001). This cellular defect causes developmental lethality in mice and multisystem disease in humans (Waterham *et al.*, 2007; Ishihara *et al.*, 2009; Wakabayashi *et al.*, 2009).

Four receptors have been identified that recruit Drp1 to mitochondria: mitochondrial fission 1 protein (Fis1), mitochondrial fission factor (Mff), and mitochondrial dynamics proteins of 49 and 51 kDa (MiD49 and MiD51, respectively; Yoon *et al.*, 2003; Gandre-Babbe and van der Bliek, 2008; Palmer *et al.*, 2011; Zhao *et al.*, 2011). Fis1, the first identified candidate receptor, has a minor role in Drp1 recruitment (Otera *et al.*, 2010; Loson *et al.*, 2013), and recent results suggest instead a role in mitophagy (Shen *et al.*, 2014; Yamano *et al.*, 2014). There is good evidence that the last three molecules are each capable of recruiting Drp1, as the loss of any of these receptors results in reduced Drp1 accumulation on mitochondria and increased mitochondrial tubule length (Palmer *et al.*, 2011; Loson *et al.*, 2013; Palmer *et al.*, 2013). Mff appears to be the primary receptor. Loss of Mff results in the greatest reduction of fission in mouse embryonic fibroblasts, whereas overexpression causes mitochondrial fragmentation consistent with increased fission rates (Otera *et al.*, 2010; Loson *et al.*, 2013). MiD51 and MiD49 both

This article was published online ahead of print in MBoC in Press (http://www.molbiolcell.org/cgi/doi/10.1091/mbc.E15-08-0591 on October 7, 2015.

Address correspondence to: David C. Chan (dchan@caltech.edu).

Abbreviations used: BSE, bundle signaling element; CC, coiled coil; Drp1, dynamin-related protein 1; Fis1, fission 1; IB, insert B; Mff, mitochondrial fission factor; MiD49/51, mitochondrial dynamics protein of 49/51 kDa; SEC, size exclusion chromatography.

Supplemental Material can be found at:
http://www.molbiolcell.org/content/suppl/2015/10/05/mbc.E15-08-0591v1.DC1.html

strongly recruit Drp1 and are associated with endoplasmic reticulum–mitochondria contact sites (Zhao *et al.*, 2011; Koirala *et al.*, 2013; Palmer *et al.*, 2013; Elgass *et al.*, 2015). However, in contrast to Mff, overexpression of MiD51 or MiD49 paradoxically results in mitochondrial elongation and inhibition of fission, presumably because they recruit an inactive form of Drp1 (Loson *et al.*, 2013; Palmer *et al.*, 2013).

An important issue is why Mff shows a different cellular behavior than MiD51 and MiD49. A route to addressing this issue is to examine the physical interaction between Drp1 and its receptors in vitro. However, such physical interactions have only been detected using cross-linking reagents, suggesting that the Drp1-receptor interactions are of low affinity or transient (Otera *et al.*, 2010; Strack and Cribbs, 2012). In yeast, the interaction between Dnm1 (the yeast orthologue of Drp1) and its receptor, Mdv1, is much more stable and has been linked to the insert B domain, which associates with the B-propeller domain of Mdv1 (Bui *et al.*, 2012). In mammals, the analogous insert B domain is a largely unstructured domain that is targeted for control by posttranslational modifications and interacts with cardiolipin to associate Drp1 with lipid membranes (Chang and Blackstone, 2010; Frohlich *et al.*, 2013; Bustillo-Zabalbeitia *et al.*, 2014; Stepanyants *et al.*, 2015). Studies show that this domain is dispensable for Drp1 hydrolysis, membrane constriction, and mitochondrial recruitment (Strack and Cribbs, 2012; Francy *et al.*, 2015). These results imply that in mammals, the Drp1–receptor interaction is not mediated through the insert B domain.

In this study, we examine the interaction between Drp1 and Mff to gain mechanistic insight into Drp1 recruitment. Using a yeast two-hybrid assay, we identify minimal interacting regions on both Mff and Drp1, with a short N-terminal fragment of Mff being sufficient to bind the Drp1 stalk domain. We find that removal of the insert B domain from Drp1 greatly enhances the Drp1–Mff interaction, resulting in a stable complex in vitro in the absence of cross-linkers. Using a mutational screen, we identify mutants of Drp1 that specifically abolish recruitment via Mff but not MiD51. Analysis of these mutants indicates that Drp1 oligomerization is required for Mff, but not MiD51 or MiD49, to physically associate with Drp1. Taken together, the results suggest that the robust fission activity of Mff stems from its ability to selectively recruit oligomerized Drp1 to the mitochondrial surface.

RESULTS

The Mff N-terminal region and the Drp1 stalk form the core interaction unit

To interrogate the Drp1–Mff interaction, we first sought to determine the minimal region of Mff necessary for binding Drp1. Comparing the polypeptide sequence of Mff from the human, mouse, fish, frog, and fly orthologues, we find several notable features (Supplemental Figure S1A). At the N-terminus, there are two repeat motifs (R1 and R2) that are required for recruiting Drp1 (Otera *et al.*, 2010), as well as a third conserved motif (R3) that has no proposed function. Beyond R1–R3, there is a disordered region (Supplemental Figure S1B), followed by a conserved coiled-coil (CC) domain required for dimerization and a C-terminal transmembrane domain (TM). Previous assays examining the Drp1–Mff interaction were hampered by the apparent transience or instability of the complex, and therefore its detection required stabilization by cross-linking agents (Gandre-Babbe and van der Bliek, 2008; Otera *et al.*, 2010; Strack and Cribbs, 2012). To detect this transient/unstable complex in the absence of cross-linkers, we developed a yeast two-hybrid interaction assay that allowed us to examine Drp1 recruitment by Mff. Initial attempts with an Mff bait truncated just N-terminal to the transmembrane segment (Figure 1A) resulted in autoactivation (Supplemental Figure S2A). We reasoned that the acidic coiled-coil domain might be responsible and deleted it to generate three MffΔCC baits based on splice variants 1, 3, and 4 (RefSeq NP_083685.2, NP_001297626.1, and NP_001297628.1, respectively) reported previously (Gandre-Babbe and van der Bliek, 2008; Figure 1, A and B). Isoform 4 (Mff4ΔCC), the shortest construct, showed the most robust interaction, followed by isoform 3 (Mff3ΔCC) and then isoform 1 (Mff1ΔCC). To determine the minimal Mff region sufficient for recruiting Drp1, we made sequential C-terminal truncations of Mff and tested them against Drp1. Truncations that ended within the predicted disordered region retained binding, whereas truncations that deleted the R3 domain resulted in complete loss of recruitment (Figure 1C). Thus, the N-terminal Mff region containing the three conserved R1–R3 motifs appeared sufficient for Drp1 binding. These results are consistent with experiments in cell culture indicating that R1 and R2 of Mff are essential for Drp1 recruitment (Otera *et al.*, 2010).

We similarly used the yeast two-hybrid assay to identify the Mff-interacting regions of Drp1. Structurally, Drp1 consists of four main domains: the GTPase domain, the bundle signaling element (BSE), the stalk region, and the insert B (IB) region (Figure 1D; Schmid and Frolov, 2011; Ferguson and De Camilli, 2012; Frohlich *et al.*, 2013; Wenger *et al.*, 2013). We tested the ability of Mff to recruit Drp1 constructs containing deletions of one or more of these domains (Figure 1E). Deleting the GTPase domain (ΔG) reduced the interaction between Mff1ΔCC and Drp1 and between Mff3ΔCC and Drp1 but did not appreciably affect recruitment by Mff4ΔCC or smaller constructs. This suggests that the GTPase domain promotes but is not required for Drp1 interaction with Mff. Drp1 constructs lacking the insert B domain (ΔIB), on the other hand, enhanced the interaction between Drp1 and Mff. The formerly weak recruitment by Mff isoforms 1 and 3 were now more robust, and new additional interactions between Drp1 and Mff fragments 1–100, 1–61, and 1–50 (weakly) were now detected. These data suggest that the insert B domain is dispensable for the Drp1–Mff interaction and is in fact inhibitory. Removing the GTPase, BSE, and insert B domains (to generate the stalk alone) did not greatly alter Drp1 interaction with Mff relative to Drp1ΔIB alone. The interaction data therefore suggest that the minimal regions required for the Drp1–Mff interaction are the Mff R1 and R2 motifs and the Drp1 stalk domain.

Removing insert B from Drp1 stabilizes the Drp1–Mff interaction in vitro

The results from our two-hybrid analysis strongly suggest that the insert B region inhibits the interaction of Drp1 with Mff. Because previous efforts to demonstrate binding between Drp1 and Mff in vitro required cross-linking (Otera *et al.*, 2010; Strack and Cribbs, 2012; Frohlich *et al.*, 2013), we wondered whether removing the insert B region might stabilize the Drp1–Mff complex. To test this idea, we constructed a glutathione *S*-transferase (GST) fusion protein containing the N-terminal 61 residues of Mff (the minimal binding fragment) and assayed its ability to bind full-length Drp1 or Drp1ΔIB in a GST pull-down assay (Figure 2A). Whereas full-length Drp1 weakly coimmunoprecipitated, Drp1ΔIB showed efficient coassociation with Mff, suggesting substantial stabilization of binding. The insert B domain of Drp1 therefore inhibits formation of a stable Drp1–Mff interaction.

We further tested whether the Mff truncations examined in the yeast two-hybrid assay could similarly interact with Drp1 and Drp1ΔIB in the assay. Consistent with previous reports, we found poor binding between full-length Drp1 and the Mff constructs, even

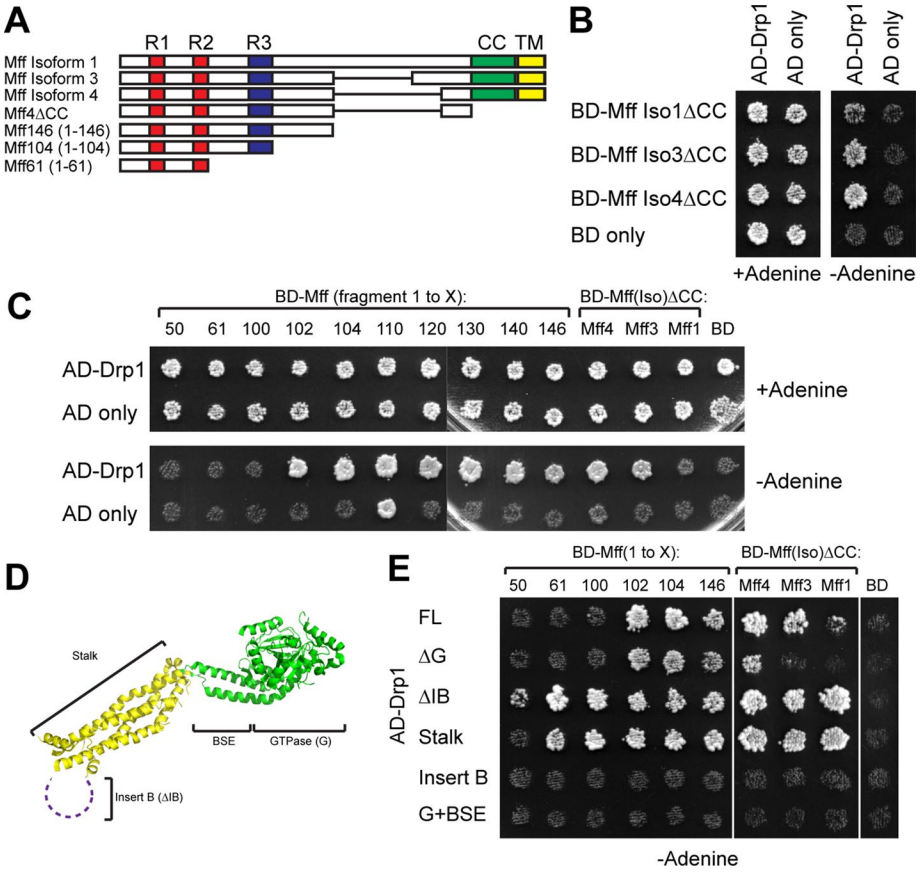

FIGURE 1: The N-terminal region of Mff binds the Drp1 stalk domain. (A) Diagram of three Mff isoforms (top three lines) and key Mff constructs (bottom four lines) used in this study. (B) Interaction of Mff isoforms 1, 3, and 4 with Drp1 in the two-hybrid assay. Mouse Mff isoforms 1, 3, and 4 with the coiled-coil domain deleted (ΔCC) were expressed from the pGBDU vector as GAL4 DNA-binding domain (BD) fusion proteins and tested against Drp1 expressed from the pGAD vector as GAL4 activation domain (AD) fusion proteins. For all two-hybrid assays in this study, growth on adenine-deficient plates indicates an interaction. The AD-only and BD-only samples are negative controls. (C) Deletion analysis of Mff. Mff fragments beginning from amino acid 1 to the number indicated above each column were expressed as BD fusion proteins and tested against Drp1 expressed as AD fusion proteins. Mff(1-110) is uninformative due to autoactivation (adenine-deficient plate shows growth with AD only). (D) Ribbon diagram of Drp1 structure, from Protein Data Bank file 4BEJ. The major domains of Drp1 are highlighted. (E) Domain analysis of Drp1. Mff truncations were expressed as BD fusion proteins and tested against Drp1 truncations expressed as AD fusion proteins. ΔG, Drp1 minus the GTPase domain; ΔIB, Drp1 minus the insert B domain; FL, full-length Drp1; G + BSE domain, GTPase plus the BSE domain; stalk, Drp1 minus the GTPase, bundle signaling element (BSE), and insert B domains. The associated diploid selection plates are shown in Supplemental Figure S2.

though such constructs show interaction in the two-hybrid assay (Figure 2B, top). In contrast, Drp1ΔIB showed robust association with Mff(1-61) and Mff(1-50) and less binding to longer constructs (Figure 2B, bottom). The larger number of interactions detected with the two-hybrid assay is consistent with the idea that the two-hybrid assay can detect weak or transient interactions (Van Criekinge and Beyaert, 1999) that are missed by biochemical assays. The pull-down results suggest that the strongest interacting pair is Drp1ΔIB and Mff(1-61). To test the stability of this interaction, we mixed Mff(1-61)–GST with Drp1ΔIB and analyzed the mixture on an analytical size-exclusion column to test for a complex (Figure 2C). Compared to Drp1ΔIB or Mff(1-61)–GST alone samples (Figure 2C, left), the mixture showed a distinct peak migrating at a higher molecular weight, concomitant with a decrease in the peaks corresponding to individual Drp1ΔIB and Mff(1-61)–GST (Figure 2C, middle and right). To determine the identity of this size-shifted species, we collected and analyzed the fractions from the size exclusion chromatography (SEC) runs and found that fractions corresponding to the new peak contained both Drp1ΔIB and Mff(1-61)–GST (Figure 2D), suggesting that Drp1ΔIB and Mff(1-61)–GST are comigrating as a complex.

Identification of Drp1 mutants that have selective loss of Mff versus MiD51 binding

The identification of the stalk region of Drp1 as the Mff-interaction domain provided us with a smaller target for determining the interacting residues on Drp1. We previously used a mutation screening strategy to identify a Drp1-interacting loop on MiD51 (Loson *et al.*, 2014). Similarly, we tested a series of Drp1 mutants for interactions with Mff in our yeast two-hybrid assay. The screening considerations were as follows: 1) we limited our mutations to surface-exposed residues of Drp1 with low homology to dynamin 2, as reasoned by the lack of an Mff interaction with dynamin 2 in our yeast two-hybrid assay (Supplemental Figure S2C); 2) we used two Mff constructs of various binding efficiency (Figure 1A) as baits to provide additional sensitivity for the screen; 3) because previous studies indicated that the yeast two-hybrid assay provides a readout of Drp1 oligomerization (Naylor *et al.*, 2006; Chang *et al.*, 2010), we included a Drp1 bait to obtain information about the oligomerization activity of the Drp1 mutants; and 4) because Mff-specific mutants were desired, we included MiD51 as a bait to screen against Drp1 mutants that also affected MiD51 binding.

We assayed 42 Drp1 mutants (Figure 3A and Supplemental Table S1) for binding to the Mff, Drp1, and MiD51 baits. Several interesting patterns emerged from the screen. All mutants that affected Drp1 oligomerization, as interpreted by loss of interaction with the Drp1 bait, also abolished binding to Mff (Figure 3A, mutants 8, 9, 15, 18, and 20). In contrast, some of these mutants retained MiD51 binding (mutants 9 and 15). Loss of Drp1 oligomerization therefore correlates tightly with loss of Mff binding but not MiD51 binding. In addition, we recovered several Drp1 mutants that failed to bind Mff but retained binding to both Drp1 and MiD51. We chose six for further study (mutants 10, 13, 16, 17, 22, and 28) and introduced them into a Drp1ΔIB background to test whether removing the insert B domain could rescue the loss of binding (Figure 3B). In three of six mutants, we found recovery of interaction with Mff, consistent with the notion that the insert B domain is inhibitory to the interaction. This secondary screen left us with three mutants that we interpret as bona fide Mff-binding mutants for further characterization (Figure 3C). We tested the three mutants in our in vitro interaction assays to validate the results of the yeast two-hybrid assay. Whereas wild-type Drp1ΔIB binds robustly to Mff(1-61), all three mutants (in the context of Drp1ΔIB) failed to

coprecipitate with Mff(1-61) by GST pull down (Figure 4A). Furthermore, by SEC analysis, these mutants showed loss of complex formation with Mff(1-61) (Figure 4B). Taken together, the data suggest that these mutants are indeed defective in Mff binding.

Drp1 mutants are defective for fission and mitochondrial recruitment and are specific to Mff versus MiD51 and MiD49

To assess the physiological function of these mutants, we expressed them in *Drp1*-null mouse embryonic fibroblasts (MEFs). Owing to loss of mitochondrial fission, *Drp1*-null MEFs have highly elongated and interconnected mitochondria. Reexpression of wild-type Drp1 restores mitochondrial fission, resulting in shorter mitochondrial tubules (Figure 5A). In contrast, expression of the three Drp1 mutants defective in Mff binding did not shorten the mitochondrial network, indicating that they are nonfunctional for fission (Figure 5A). To understand this defect, we assessed whether localization of the Drp1 mutants to mitochondria was impaired. Because the strong cytosolic signal of overexpressed Drp1 obscured this analysis, we briefly permeabilized the cells with digitonin to remove soluble Drp1 before immunostaining. This treatment artifactually resulted in mitochondrial fragmentation but greatly improved the visualization of Drp1 complexes on the mitochondria (Figure 5B). In wild-type cells, there is a substantial amount of endogenous Drp1 localized to mitochondria. In *Mff*-null cells, there is little Drp1 on mitochondria, consistent with its role as the major Drp1 recruiter (Otera *et al.*, 2010; Loson *et al.*, 2013). When wild-type Drp1 is expressed in *Drp1*-null cells, there is robust recruitment of Drp1 on the mitochondria (Figure 5B, magnification insets). In contrast, the three Mff-binding mutants show a major loss of Drp1 puncta on mitochondria (Figure 5B, magnification insets). Mutant 17 appears to form aggregates in the cell, but the majority of these aggregates did not colocalize with mitochondria.

To determine whether these mutants are selectively defective for Mff binding, we tested their recruitment by ectopically targeted Mff, MiD51, and MiD49. FLAG-tagged versions of the three Drp1 receptors were targeted to lysosomes by fusion to lysosomal-associated membrane protein 1 (LAMP1). These constructs were expressed in *Drp1*-null cells, and localization of wild-type Drp1 versus mutant Drp1 was assessed (Figure 6). When wild-type Drp1 was expressed, it was robustly recruited to FLAG-positive puncta in the Mff-, MiD51-, and MiD49-expressing cell lines (Figure 6A). When the three Drp1 mutants were expressed, they strongly localized to FLAG-positive puncta in the lysosome-targeted MiD51 and MiD49 cell lines but not in the lysosome-targeted Mff cell line (Figure 6, B–D). Taken together, the data suggest that mutants 10, 16, and 17 specifically disrupt the interaction of Drp1 with Mff but not MiD49 or MiD51 and that the major observed reduction of Drp1 puncta on mitochondria (Figure 5B) can be attributed specifically to loss of Mff-mediated recruitment.

Oligomerization-dependent recruitment of Drp1 by Mff

In our two-hybrid screen for Drp1 mutants defective for Mff binding, we explicitly screened against mutants that had defects in oligomerization and ultimately recovered three mutants that fulfilled our criteria. However, the results from the screen suggested that Drp1 oligomerization is tightly associated with its ability to bind Mff, as every Drp1 mutant defective in oligomerization is also deficient in Mff binding. We therefore wondered whether the identified mutants (10, 16, and 17) might have a moderate oligomerization defect that was not detectable in the yeast two-hybrid assay. This concern was increased by the observation that the mutated residues are located adjacent to known oligomerization loops for Drp1 and dynamin (Figure 3C; Frohlich *et al.*, 2013; Reubold *et al.*, 2015). For these reasons, we considered the possibility that the yeast two-hybrid screen may not have provided a sufficiently stringent filter against oligomerization mutants. We therefore performed two independent tests of oligomerization activity to assess the behavior of the mutants against that of wild type and a mutant termed 4A (the four residues 401GPRP404 mutated to AAAA) that forms dimers but cannot form tetramers or higher-order oligomers (Frohlich *et al.*, 2013). In a GTPγS-stimulated assembly assay, ~50% of Drp1 sediments when incubated in 50 mM NaCl (Figure 7A). In contrast, the 4A mutant is almost completely deficient in assembly and remains highly soluble. Mutants 16 and 17 sedimented substantially less than wild-type Drp1 but more than the dimeric 4A mutant. Mutant 10 did not show a clear sedimentation defect. Under low-salt conditions that promote oligomerization, SEC analysis of the mutants showed that mutants 10, 16, and 17 all migrated substantially more slowly than wild type, indicating a defect in forming higher-order oligomers (Figure 7B). Mutant 17 migrated similarly to the 4A mutant, whereas mutants 10 and 16 showed a somewhat less pronounced defect. Taken together, the results suggest that all three mutants can form dimers but are inefficient at further oligomerization, although the defects are not as strong as for the canonical 4A oligomerization mutant.

If Drp1 oligomerization is necessary for Mff binding, then our model predicts that the 4A mutant would be unable to bind Mff. To test this, we examined the mutant in the yeast two-hybrid assay (Figure 7C), the GST pull-down assay (Figure 7D), and the complex formation assay (Figure 7E). Consistent with our model, the 4A mutant showed strong defects in Mff association in all assays. Of importance, the two-hybrid assay showed that 4A had normal binding to MiD51.

DISCUSSION

Mff is likely to be the major Drp1 receptor. Cells lacking Mff, compared with the other receptors (Fis1, MiD51, MiD49), show the most highly elongated mitochondria (Otera *et al.*, 2010; Loson *et al.*, 2013). However, the lack of a stable interaction between the two proteins in vitro has been puzzling. Here, we show that recombinant Drp1 lacking the insert B region, unlike full-length Drp1, forms a stable complex with the N-terminal region of Mff. This observation indicates that insert B inhibits Drp1 binding to Mff. In contrast to the mammalian situation, insert B in yeast Dnm1 has been shown to promote binding to the Mdv1/Fis1 receptor complex (Bui *et al.*, 2012). It is tempting to speculate that the mammalian Drp1 insert B domain may regulate mitochondrial fission by dampening Drp1–Mff interactions until signals to activate fission are present. To understand this issue, it will be important to determine how the inhibitory effect of insert B on Mff binding is modulated. Because insert B has been shown to interact with cardiolipin (Bustillo-Zabalbeitia *et al.*, 2014; Macdonald *et al.*, 2014; Ugarte-Uribe *et al.*, 2014; Stepanyants *et al.*, 2015), the possible role of lipids in regulating Drp1–Mff interactions should be tested. In addition, it is interesting to note that insert B contains residues are targeted for phosphorylation and sumoylation (Figueroa-Romero *et al.*, 2009; Chang and Blackstone, 2010). Phosphorylation of serine 616 in human Drp1 (corresponding to serine 579 in mouse Drp1) activates its fission activity (Taguchi *et al.*, 2007; Kashatus *et al.*, 2011). This serine residue resides in insert B, but phosphomimetic mutants of this residue do not increase the binding of full-length Drp1 to Mff in vitro (Supplemental Figure S3).

Our analysis of Drp1 mutants that are deficient for Mff binding suggests that the oligomerization state of Drp1 is closely

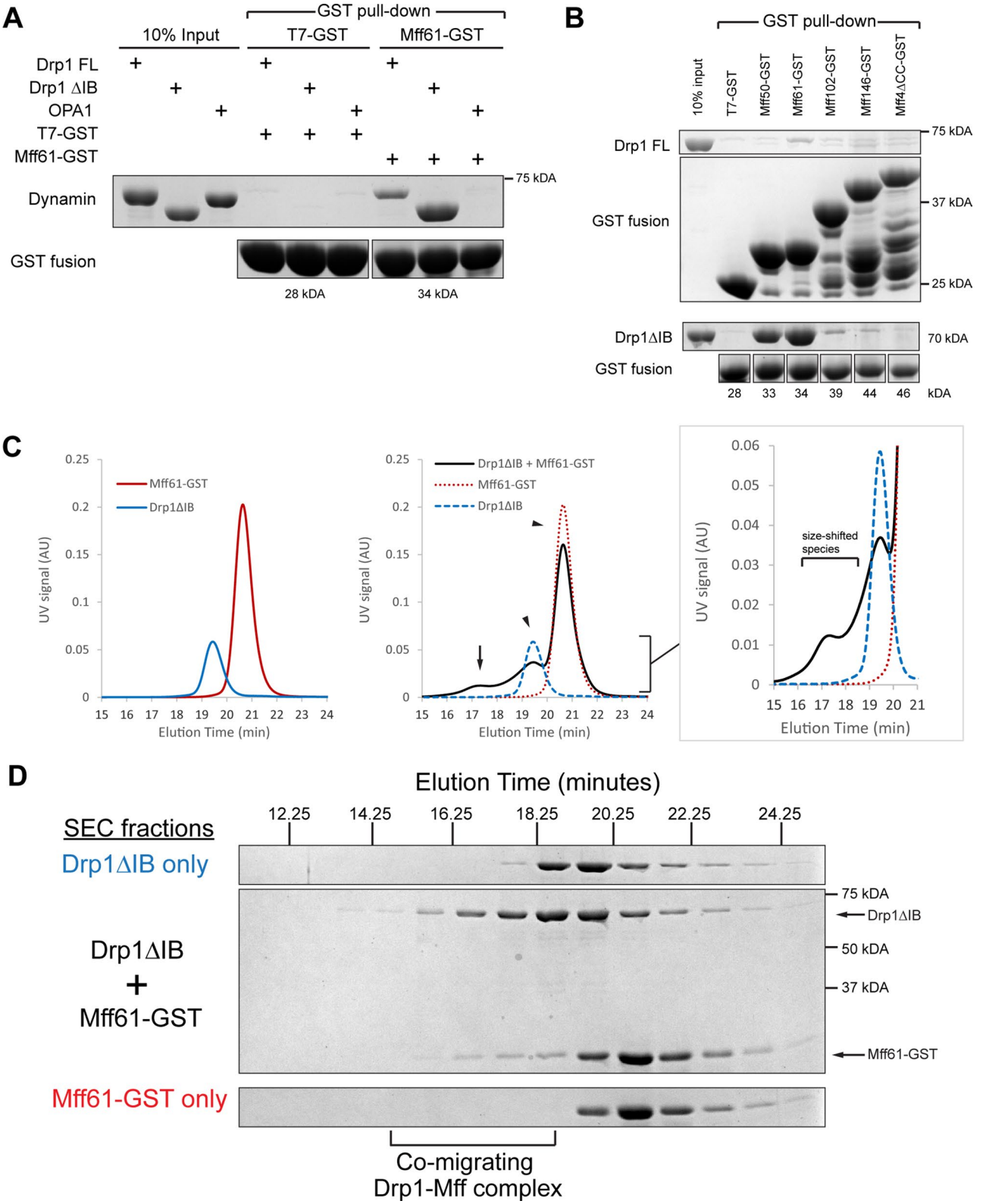

FIGURE 2: Mff61 and Drp1ΔIB form a stable complex. (A) GST pull-down assays for purified recombinant Drp1 (full-length), Drp1ΔIB, or OPA1 vs. purified recombinant Mff61-GST (Mff fragment 1–61 fused C-terminally to GST) or T7-GST (T7tag fused to GST). Coomassie-stained bands of either the input protein (lanes 1–3) or eluates from the pull downs (lanes 4–9) after separation by SDS–PAGE. In lanes 4–9, the bottom row shows the isolated GST fusion proteins. The top row depicts the coimmunoprecipitated proteins. (B) GST pull-down assays for purified recombinant full-length Drp1 (top) or Drp1ΔIB (bottom) vs. purified recombinant Mff truncations. Coomassie-stained bands of the input Drp1ΔIB or full-length Drp1 proteins (lane 1) and eluates from the pull downs (lanes 2–7) after separation by SDS–PAGE. The Drp1ΔIB or Drp1 FL row depicts the respective proteins pulled down by the GST fusion proteins in the lower row. (C) SEC analyses of Drp1ΔIB and Mff61-GST. Left, ultraviolet (UV) absorbance profiles of elutions from SEC run of either

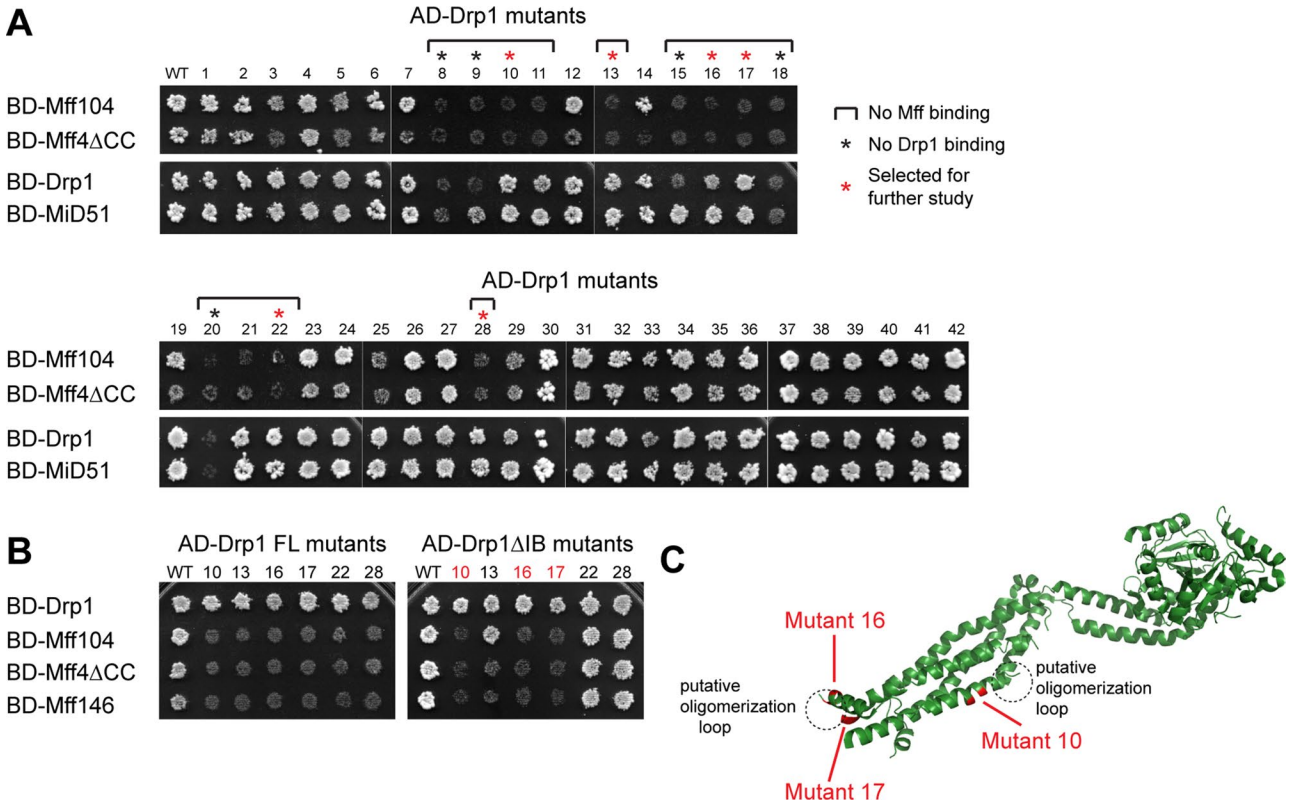

FIGURE 3: Identification of Drp1 mutants that fail to bind Mff. (A) Screen of Drp1 mutants by the yeast two-hybrid assay. Full-length Drp1 and Drp1 mutants 1–42 (see Supplemental Table S1) were expressed as AD fusion proteins and tested against Mff104 (Mff fragment 1–104), Mff isoform 4 with its coiled-coil domain deleted (Mff4ΔCC), full-length Drp1, and MiD51 expressed as BD fusions. The adenine-deficient plates are shown. The associated diploid selection plates are shown in Supplemental Figure S2. Brackets indicate Drp1 mutants that did not interact with Mff, black asterisks denote Drp1 mutants that did not interact with Drp1 (indicating loss of oligomerization ability), and red asterisks denote the subset of Mff-binding–deficient mutants that were selected for further characterization. (B) Secondary screen for Drp1 mutants. The indicated Drp1 mutants were screened against full-length Drp1, Mff104, Mff4ΔCC, and Mff146 (Mff fragment 1–146). The Drp1 mutants were constructed in full-length Drp1 (FL) and Drp1ΔIB. The adenine-deficient plates are shown. The associated diploid selection plates are shown in Supplemental Figure S2. Mutants highlighted in red from the Drp1ΔIB assay were selected for further characterization. (C) Location of mutations 10, 16, and 17 indicated on the structure of Drp1 (Protein Data Bank file 4BEJ). Loops implicated in higher-order assembly of Drp1 are marked.

linked to its interaction with Mff. In the cytosol, Drp1 exists in a dimer/tetramer/high-order equilibrium, with data supporting either tetramers or dimers as the predominant species (Zhu *et al.*, 2004; Koirala *et al.*, 2013; Macdonald *et al.*, 2014). Our mutational screen shows that Mff is unable to stably associate with Drp1 that is oligomerization defective. Of importance, our mutations do not disrupt the Drp1 monomer:monomer interaction surface (termed "interface 2") in the stalk region that is important for formation of the cross-like stalk dimer (Ferguson and De Camilli, 2012; Frohlich *et al.*, 2013). Like the 4A mutant, mutants 10, 16, and 17 are all capable of forming dimers but are defective in formation of higher-order states. Therefore it appears that the Drp1 oligomeric state recruited by Mff is a tetramer or higher. In contrast, MiD51 and MiD49 do not show this strong requirement for Drp1 oligomerization.

Two general models can explain why Mff strongly prefers a higher-order state of Drp1. For simplicity in presenting the models, we assume that Mff binds to a Drp1 tetramer, although the

purified recombinant Mff61-GST alone (red) or purified recombinant Drp1ΔIB alone (blue). Middle, UV absorbance profile of elutions from SEC run of Mff61-GST and Drp1ΔIB preincubated together for 1 h before loading overlaid on top of the profiles on the left. Arrowheads depict a loss of Mff61-GST and Drp1ΔIB UV signal in the mixed sample. The arrow depicts the formation of a new peak eluting at an earlier time, indicating the formation of higher–molecular weight species. Right, magnification of a portion of the middle graph to highlight the size-shifted species of the new peak (underneath the bracket) from the Mff61-GST + Drp1ΔIB run. (D) SDS–PAGE analysis of fractions collected from the SEC runs in C. Fractions from the times indicated at the top were collected from the SEC runs in C, resolved by SDS–PAGE, and Coomassie stained. Top, Drp1ΔIB bands from the Drp1ΔIB- only run; middle, Drp1ΔIB and Mff61-GST bands (arrows) from the combined run; bottom, Mff61-GST bands from the Mff61-GST–only run. The brackets highlight the presence of both Drp1ΔIB and Mff61-GST in the combined run not present in the individual runs, indicating a Drp1–Mff complex.

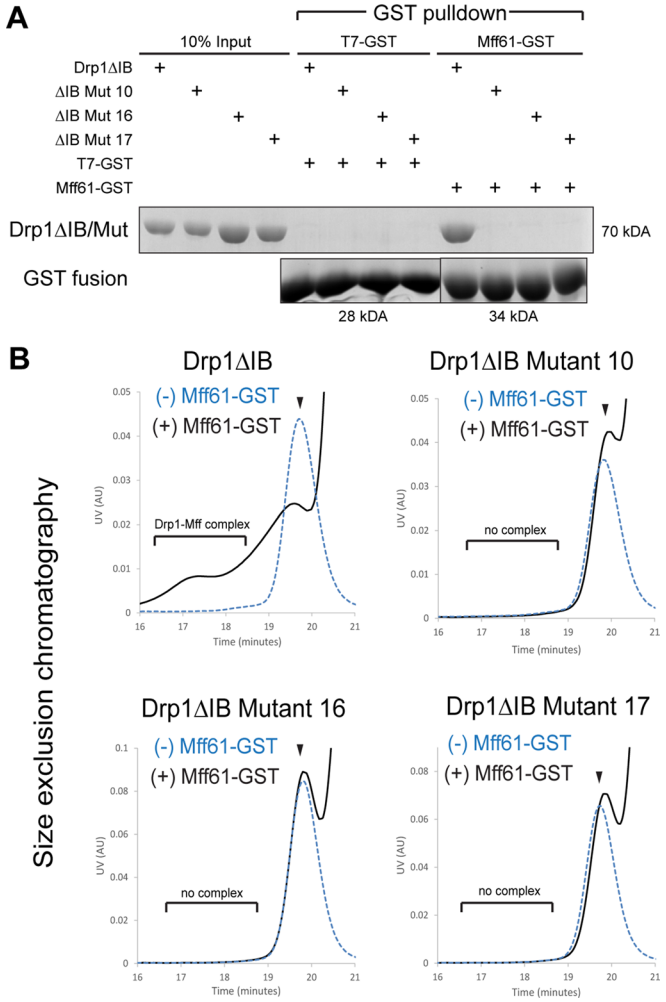

FIGURE 4: Drp1 mutants display loss of interaction with Mff in vitro. (A) GST pull-down assays for purified recombinant Drp1 variants against purified recombinant Mff61-GST or T7-GST. Coomassie-stained bands of either the input protein (10% input lanes) or eluates from the pull downs (GST pull-down lanes) after separation by SDS–PAGE. The top row (lanes 5–12) depicts the Drp1 proteins pulled down by the GST fusion proteins in the bottom row. (B) SEC analyses of Mff61-GST with Drp1ΔIB and Drp1ΔIB mutants. For Drp1ΔIB and each mutant, two SEC runs were performed, one with Mff61-GST and one without it. Depicted are overlays of the UV absorbance profiles from the two separate runs. The brackets highlight the elution time during which the Drp1–Mff complex appears in the Drp1ΔIB (wild type) + Mff61-GST run. This complex is absent in runs with the Drp1 mutants. The arrowhead highlights the reduction in Drp1 signal from the combined run relative to the original peak position in the Drp1ΔIB-alone runs (dotted). The corresponding signals in the mutant samples do not show a decrease.

bound form may be a larger assembly. In the first model, the Mff-binding site is generated only when two Drp1 dimers form a tetramer. The cross-like Drp1 dimers come together through apposition of their stalk domains, forming a new surface that is now directly recognized by the N-terminal region of Mff. In the second model, the Mff-binding surface exists in the Drp1 dimer, but formation of the Drp1 dimer:dimer complex is required for stability. In both cases, the functional result is that only the oligomerized form of Drp1 is recruited, whereas Drp1 dimers are left in the cytosol. Both models are consistent with the observation that the Mff-binding unit consists of the Drp1 stalk, which contains the interfaces supporting Drp1 tetramerization (Frohlich *et al.*, 2013; Francy *et al.*, 2015; Reubold *et al.*, 2015). Because Mff has a coiled-coil domain, it is also possible that Mff dimerization may facilitate formation of additional Drp1–Drp1 interactions. In yeast, Mdv1 functions to nucleate Dnm1 assembly (Lackner *et al.*, 2009).

In binding only to higher-order Drp1 oligomers, Mff differs strikingly from MiD51 and MiD49. Our studies show that the last two proteins are still able to bind Drp1 mutants that can only form dimers. In this regard, the Drp1–MiD interaction resembles that of yeast Dnm1–Mdv1, which is not affected by oligomerization-defective mutations in Dnm1 (Ingerman *et al.*, 2005; Bhar *et al.*, 2006). These results underscore a major difference between Mff- and MiD-mediated recruitment and may explain their distinct cellular effects. In cells, overexpressed Mff results in increased fission (Otera *et al.*, 2010). In contrast, overexpressed MiD51 or MiD49 results in high accumulation of Drp1 on mitochondria, but the net effect is reduced fission and mitochondrial elongation because the recruited Drp1 is inactive (Loson *et al.*, 2013; Palmer *et al.*, 2013). We speculate that by selectively recruiting the subpopulation of Drp1 that is oligomeric, Mff might be recruiting an active pool of Drp1 that is fission competent. In contrast, the MiDs appear to recruit an inactive Drp1 population, including dimers, that requires an additional trigger before fission induction (Figure 7F).

MATERIALS AND METHODS

Cloning for protein expression

Mouse Drp1 isoform b (699 amino acids), Drp1ΔIB (1–513 fused to 603–699), Drp1ΔIB 4A (401GPRP404 mutated to AAAA), and Drp1 mutants 10, 16, and 17 (mutations described in Supplemental Table S1) were cloned into the *Nde*I and *Bam*HI sites of a modified pET21b+ vector containing a downstream PreScission Protease cleavage site (EMD Millipore, Billerica, MA). Mouse Mff isoform 4ΔCC, Mff(1-50), Mff(1-61), Mff(1-102), and Mff(1-146) were cloned into the *Nde*I and *Bam*HI sites of a modified pET28a(+) vector containing a downstream PreScission Protease cleavage site and GST tag (EMD Millipore). The parental vector, which produces a tagged GST, was used to express the T7-GST negative control used in GST pull-down assays. OPA1 (262–1015, isoform 8), used as a negative control in GST pull-down assays, was cloned into a modified pET28a(+) vector with an upstream PreScission Protease site. Mutants were generated by overlap PCR mutagenesis and verified by sequencing.

Protein expression and purification

Recombinant protein was expressed in Rosetta (DE3) BL21 *Escherichia coli* (EMD Millipore). Transformed bacteria were grown in 1 l of terrific broth containing 25 μg/ml chloramphenicol and either 100 μg/ml ampicillin (pET21 vectors) or 50 μg/ml kanamycin (pET28 vectors) at 37°C to an OD_{600} of 1.5, shifted to 16°C, and induced with 0.5 mM isopropyl β-D-1-thiogalactopyranoside for overnight expression, typically 18 h. Cells were harvested, and pellets were stored at –20°C. For hexahistidine-tagged proteins, cell pellets were thawed and resuspended in buffer containing 25 mM 4-(2-hydroxyethyl)-1-piperazineethanesulfonic acid (HEPES), pH 7.8, 500 mM NaCl, 10% glycerol, and 5 mM β-mercaptoethanol (β-Me; His lysis buffer) plus 5 mM imidazole and 1× HALT protease inhibitors (Thermo-Pierce, Rockford, IL), lysed by sonication, and cleared by centrifugation at 43,000 × *g* for 30 min at 4°C. Supernatant was applied to 1-ml bed volume of washed Talon beads (Clontech, Mountain View, CA) for 3 h, washed with His lysis buffer plus 20 mM imidazole, and exchanged

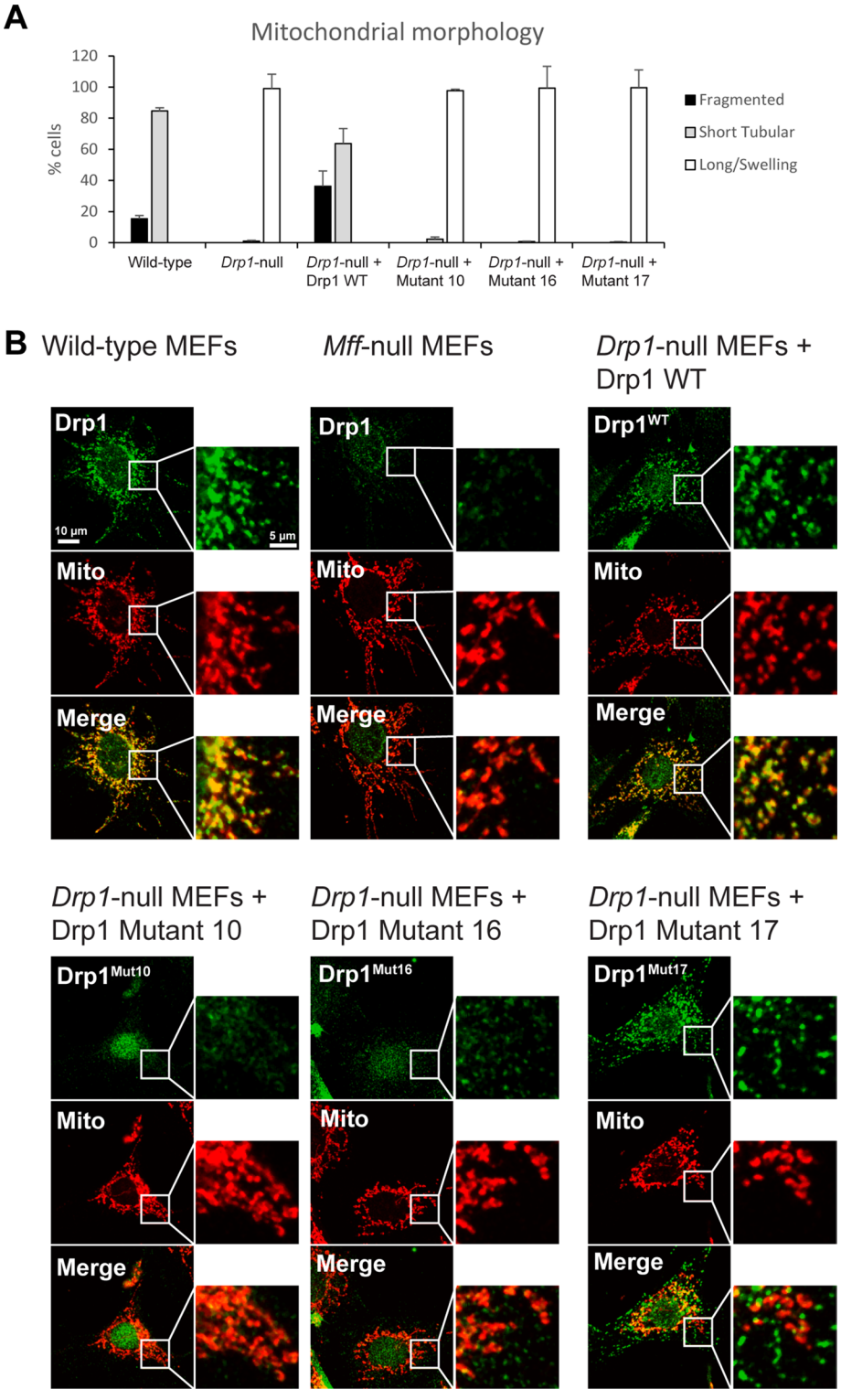

FIGURE 5: Drp1 mutants lack fission activity and are not recruited to mitochondria. (A) Fission activity upon expression in *Drp1*-null MEFs. Wild-type MEFs, *Drp1*-null MEFs, and *Drp1*-null MEFs expressing wild-type Drp1, Drp1 mutant 10, Drp1 mutant 16, or mutant 17 were immunostained against Tom20 to visualize their mitochondrial morphology and scored into three categories: fragmented, short tubular, or elongated with swelled mitochondria. Quantitation was done in triplicate, with 100 cells scored per experiment. Error bars, SEM. (B) Analysis of Drp1 recruitment to mitochondria. The cell lines indicated were briefly permeabilized with digitonin to clear cytosolic Drp1 before fixation. Mitochondria were fragmented in the process, but Drp1 puncta remained on mitochondria for visualization by immunostaining with an antibody against Drp1 (Drp1, green). Mitochondria were visualized by immunostaining against the outer membrane protein Tom20 (Mito, red). Cells were imaged and images were processed under identical settings to properly assess changes in Drp1 levels from cell to cell. The Drp1 signal, mitochondrial signal, and merged signals are shown. Squares to the right are magnifications of the boxed region in the main image.

into buffer containing 20 mM HEPES, pH 7.5, 300 mM NaCl, 10% glycerol, 2 mM β-Me for overnight cleavage (typically 20 h) with 60 U of PreScission Protease (GE Healthcare, Piscataway, NJ). After cleavage, glutathione–Sepharose 4B beads (GE Healthcare) were added to remove the PreScission Protease and elutions were loaded onto a HiLoad Superdex 200 16/60 column (GE Healthcare) driven by an AKTA Purifier (GE Healthcare) and preequilibrated with buffer containing 20 mM HEPES, pH 7.5, 300 mM NaCl, 5% glycerol, and 5 mM β-Me for SEC purification. Peak fractions were collected and concentrated in Amicon-Ultra 15 concentrators, 50 MWCO (EMD Millipore). Proteins were flash frozen and stored at –80°C. For Mff-GST proteins, lysis, coupling to glutathione–Sepharose beads, and washes were performed in buffer containing 20 mM HEPES, pH 7.5, 300 mM NaCl, 10% glycerol, and 5 mM β-Me. GST fusion proteins were eluted with 10 mM reduced glutathione (Sigma-Aldrich, St. Louis, MO) in buffer containing 20 mM HEPES, pH 7.5, 150 mM NaCl, 10% glycerol, and 5 mM β-Me, desalted with Zeba desalting columns, 7 MWCO (Life Technologies, Carlsbad, CA), preequilibrated with buffer without glutathione, flash frozen, and stored at –80°C. For the Drp1–Mff comigration SEC assays, Mff(1-61)–GST was additionally purified by SEC as described, with peak fractions collected and concentrated in Amicon Ultra 15 concentrators, 30 MWCO, before freezing and storage at –80°C.

Yeast two-hybrid assay

The Drp1 constructs in Figure 1E consist of the following truncations and fusions: FL, full-length Drp1, amino acids (aa) 1–699; ΔG, Drp1 minus the GTPase domain, aa 309–667; ΔIB, Drp1 minus the insert B domain, aa 1–508 fused to 605–699 with a GGGSGGS linker; stalk, Drp1 minus the GTPase, BSE, and insert B domains, aa 329–508 fused to 605–662 with a GGGSGGS linker; insert B domain, aa 493–605; and G + BSE domain, aa 1–328 fused to 674–699 with a KHGTDSRV linker (Chappie *et al.*, 2010). Mouse dynamin 2, Drp1

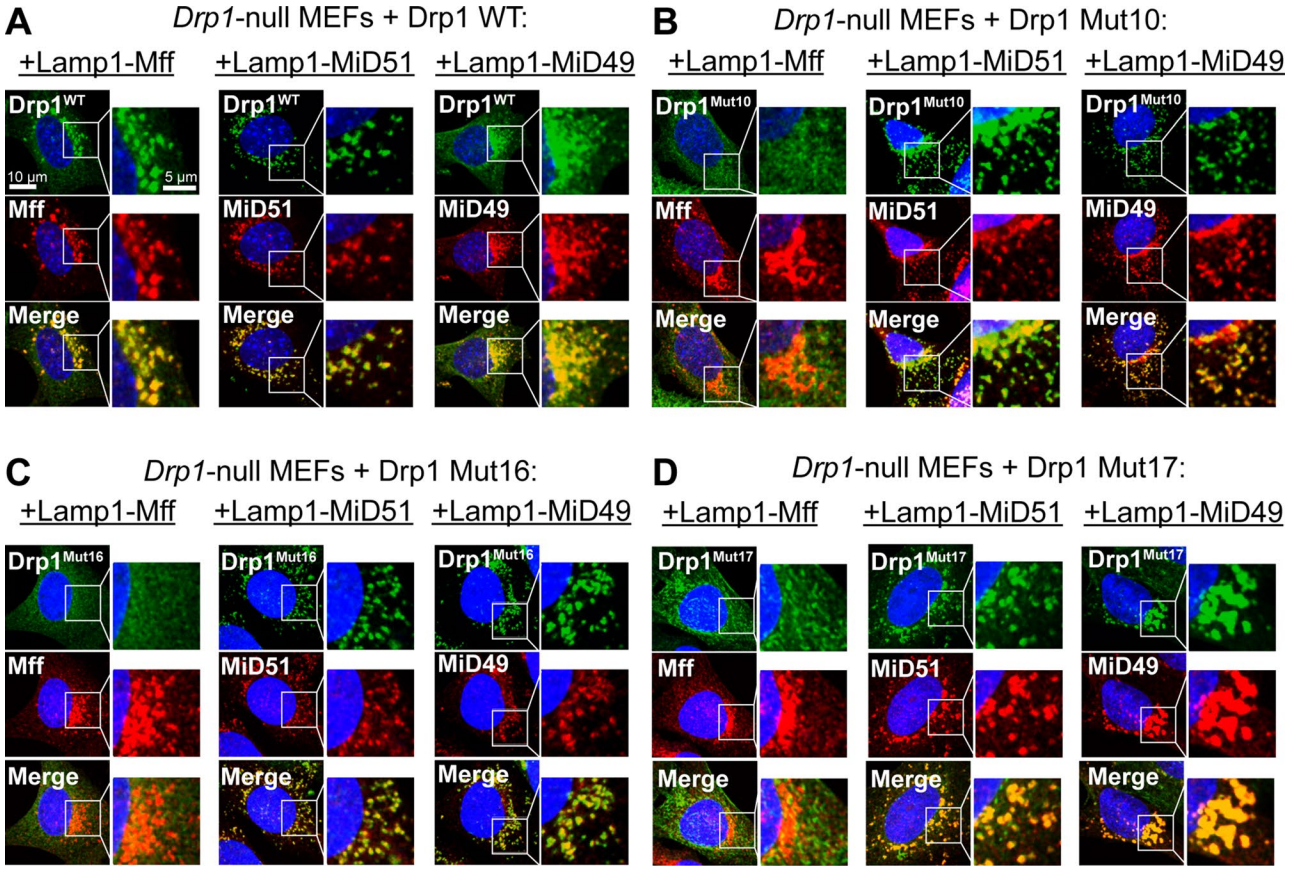

FIGURE 6: Drp1 mutants are recruited by MiD51 and MiD49 but not Mff. (A–D) FLAG-tagged Mff isoform 4, MiD51Δ, and MiD49 were targeted to lysosomes by fusion with LAMP1 in *Drp1*-null cells expressing wild-type (A) or mutant (B–D) Drp1. These cells were fixed and immunostained against Drp1 (green) and FLAG (red) for assessment of colocalization. The boxed regions are magnified.

isoform b, Drp1ΔIB 4A, Drp1 truncations and mutants in Figure 1E and Supplemental Table S1, and MiD51 (47–463), MffΔTM (Δ272–291), MffΔCC (Δ235–291), and Mff truncations in Figure 1C were cloned (into either the pGAD-C1 or pGBDU-C1 vectors) and transformed into PJ69-4α and PJ69-4a yeast strains, respectively. Transformants were selected with leucine- and uracil-deficient plates, respectively, and haploid combinations for interaction testing were mated by spotting on yeast extract/peptone/dextrose plus adenine plates. Diploids were selected by replica plating onto leucine- and uracil-deficient plates (labeled as +Adenine on the figures), and interactions were assayed after replica plating on leucine-, uracil-, and adenine-deficient plates (labeled as –Adenine on the figures). Growth on adenine-deficient plates indicates a positive interaction, and interaction tests were performed at least three times. Mutants were generated by overlap PCR mutagenesis and verified by sequencing. Residues for the mutational screen were selected from the set of accessible surface area residues as determined by the Surface Residues function in PyMOL, using a solvent radius of 2.5 Å applied to the structure of Drp1 (Protein Data Bank file 4BEJ).

GST precipitation assays

Each GST-fusion and target protein pair was incubated with washed glutathione–Sepharose beads in buffer containing 20 mM HEPES, pH 7.5, 150 mM NaCl, 10% glycerol, 0.1% Triton X-100, 2 mM $MgCl_2$, and 5 mM β-Me at room temperature for 1 h. The beads were washed twice with buffer, and the bound fraction was analyzed by SDS–PAGE, followed by Coomassie staining. For target proteins, 10% of the input amount is shown.

Cell lines and cell culture

All cell lines were cultured in DMEM containing 10% fetal bovine serum, 100 IU/ml streptomycin, and 100 μg/ml penicillin. *Mff*-null cell lines were previously published (Loson *et al.*, 2013). *Drp1*-null cell lines were a generous gift from Katsuyoshi Mihara (Kyushu University, Fukuoka, Japan). *Drp1*-null cells lines stably expressing Drp1 and Drp1 mutants were generated by retroviral transduction of pQCXIP (Clontech) vectors with Kozak-Drp1 cloned into the *Bam*HI/*Eco*RI sites and maintained in 0.5 μg/ml puromycin.

To generate the LAMP1 constructs, the Kozak sequence and FLAG-tag-Strep-tagII was fused to the rat Lamp1 sequence to generate a Kozak-LAMP1-FLAG construct, which was then fused to the N-terminus of Mff, MiD51, and MiD49. LAMP1-FLAG-Mff isoform 4 ΔTM (Δ272–291), LAMP1-FLAG-MiD51 (134–463), and LAMP1-FLAG-MiD49 (124–454) were cloned into the *Xho*I/*Hpa*I sites of pMSCVhyg (Clontech), retrovirally transduced into *Drp1*-null cell lines expressing Drp1 or Drp1 mutants, and maintained in 0.5 μg/ml puromycin and 100 μg/ml hygromycin.

Immunofluorescence and imaging

For immunostaining, antibodies to Drp1 (mouse anti-Dlp1; BD Biosciences, San Diego, CA), Tom20 (rabbit anti-Tom20; Santa Cruz Biotechnology, Santa Cruz, CA), and FLAG (rabbit anti-FLAG; Sigma-Aldrich) were used. Cells were grown in LabTek chambered

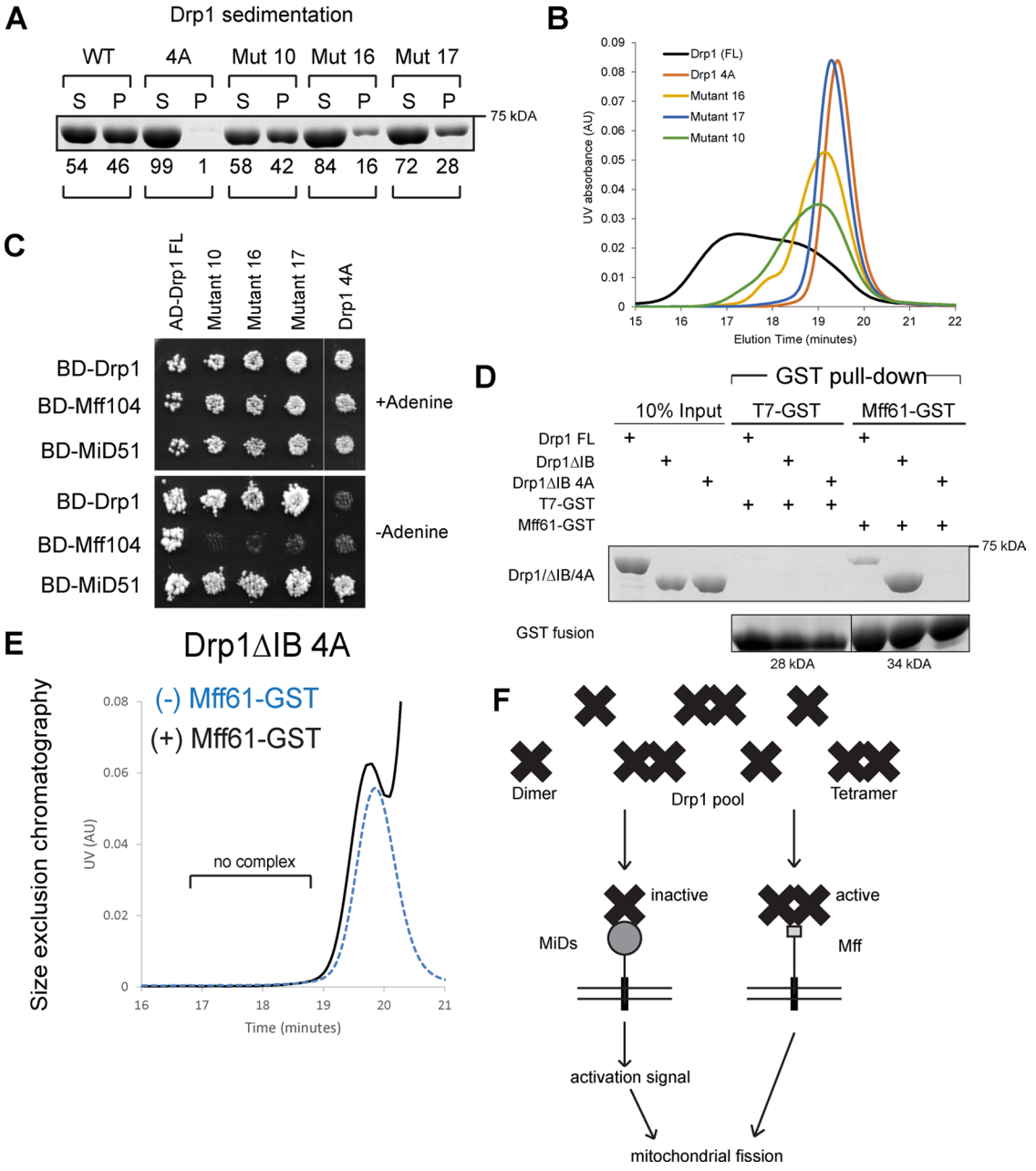

FIGURE 7: Drp1 oligomerization is required for binding to Mff. (A) Sedimentation analysis of Drp1 assembly. Purified recombinant full-length Drp1, mutants 10, 16, and 17, and the oligomerization mutant 4A were incubated with GTPγS in 50 mM salt for 30 min. Assembled Drp1 was pelleted by sedimentation at 100,000 × *g*. Equivalent volumes of the supernatant (S) and pellet (P) were loaded and resolved by SDS–PAGE. Numbers below show the percentages in the supernatant and pellet, based on densitometry measurements. (B) SEC analysis of full-length Drp1 and mutants. Purified recombinant full-length Drp1, mutants 10, 16, and 17, and the oligomerization mutant 4A were analyzed by SEC under medium-salt conditions (100 mM NaCl) to assess their ability to form higher-order oligomers. Mutant 4A (red) is known to run as a dimer. Proteins eluting before this peak are considered to represent higher-order oligomers. (C) Analysis of the 4A mutant by the yeast two-hybrid assay. Drp1, Mff104, and MiD51 were expressed as BD fusion proteins and tested against Drp1, mutants 10, 16, and 17, and the oligomerization mutant 4A expressed as AD fusion proteins. (D) Analysis of the 4A mutant by GST pull down. Coomassie-stained bands of either the input protein (10% input lanes) or eluates from the pull downs (GST pull down, lanes 4–9) after separation by SDS–PAGE. The top row depicts the Drp1 protein pulled down by the GST fusion proteins in the bottom row. (E) Analysis of the 4A mutant by SEC. Overlays from SEC runs of the 4A mutant with and without Mff61-GST. The brackets highlight the absence of a Drp1-Mff complex at the expected elution time (compare to Figure 4B). (F) Model of differential recruitment of Drp1 by Mff vs. MiD51 and MiD49. Drp1 exists in the cytosol as a pool of dimers (cross) and tetramers (two adjacent crosses). Whereas MiD51 and MiD49 (MiDs; left) can recruit Drp1 dimers, Mff (right) requires oligomerization of Drp1 dimers. The Drp1 recruited by MiD51 and MiD49 remains inactive unless additional cellular signals are triggered. For simplicity, Mff is depicted as recruiting tetramers, but it is possible that the recruited form of Drp1 is in a higher assembly state.

glass slides (Nunc, Rochester, NY) for fixed-cell imaging. Cells were fixed in prewarmed 4% formaldehyde for 10 min at 37°C, permeabilized in 0.1% Triton X-100, and incubated with antibodies in 5% fetal calf serum, all in phosphate-buffered saline. For cytosol clearing of soluble Drp1, cells were permeabilized with 0.005% digitonin in buffer containing 20 mM HEPES, pH 7.3, 110 mM potassium acetate, 2 mM magnesium acetate, 0.5 mM ethylene glycol tetraacetic acid, 220 mM mannitol, 70 mM sucrose, and 2 mM fresh dithiothreitol for 90 s at room temperature and then fixed and immunostained as described. Scoring of mitochondrial morphology was performed blind to genotype in triplicates of 100 cells. Imaging was performed with a Plan-Apochromat 63×/1.4 oil objective on a Zeiss LSM 710 confocal microscope driven by Zen 2009 software (Carl Zeiss, Jena, Germany). Images were cropped, globally adjusted for contrast and brightness, and median filtered using ImageJ (National Institutes of Health, Bethesda, MD).

Size exclusion chromatography

For the analysis of Drp1–Mff complex formation, 80 µg of Drp1ΔIB/ mutants and 80 µg of Mff(1-61)–GST were incubated separately or together in 100 µl of 20 mM HEPES, pH 7.5, 150 mM NaCl, 10% glycerol, 2 mM $MgCl_2$, and 5 mM β-Me for 1 h at room temperature, filtered through a 0.1-µm Durapore filter column (EMD Millipore), and loaded onto a Shodex KW804 column (Wyatt Technology, Goleta, CA) driven by a Varian HPLC (Varian, Palo Alto, CA) at 0.5 ml/min. Fractions were collected manually at 1-min intervals. For analysis of oligomerization, 12.5 µM Drp1 was incubated in the foregoing buffer at 100 mM NaCl before loading onto the column.

Pelleting assay

Drp1 or mutants at 15 µM were incubated in buffer containing 20 mM HEPES, pH 7.5, 50 mM NaCl, 2 mM $MgCl_2$, 5 mM β-Me, and 1 mM GTPγS for 30 min at room temperature and then centrifuged at 100,000 × *g* with a TLA100.3 rotor in a Beckman Optima MAX Ultracentrifuge for 20 min at 22°C. Supernatants were removed, and the pellet was resuspended in an equal volume of buffer. Equal amounts of supernatant and pellets were analyzed by SDS–PAGE, followed by Coomassie staining.

Sequence alignments and analysis

Sequence alignments were performed with MultAlin (Corpet, 1988) and formatted with ESPript (Robert and Gouet, 2014). Disorder prediction was performed with DisMeta (Huang *et al.*, 2014).

ACKNOWLEDGMENTS

We are grateful to Katsuyoshi Mihara for the *Drp1*-null MEFs. R.L. was supported by a National Science Foundation Graduate Research Fellowship Program Award (1144469). This work was supported by National Institutes of Health RO1 Grant GM110039.

REFERENCES

Bhar D, Karren MA, Babst M, Shaw JM (2006). Dimeric Dnm1-G385D interacts with Mdv1 on mitochondria and can be stimulated to assemble into fission complexes containing Mdv1 and Fis1. J Biol Chem 281, 17312–17320.

Bui HT, Karren MA, Bhar D, Shaw JM (2012). A novel motif in the yeast mitochondrial dynamin Dnm1 is essential for adaptor binding and membrane recruitment. J Cell Biol 199, 613–622.

Bustillo-Zabalbeitia I, Montessuit S, Raemy E, Basanez G, Terrones O, Martinou JC (2014). Specific interaction with cardiolipin triggers functional activation of Dynamin-Related Protein 1. PLoS One 9, e102738.

Chan DC (2012). Fusion and fission: interlinked processes critical for mitochondrial health. Annu Rev Genet 46, 265–287.

Chang CR, Blackstone C (2010). Dynamic regulation of mitochondrial fission through modification of the dynamin-related protein Drp1. Ann NY Acad Sci 1201, 34–39.

Chang CR, Manlandro CM, Arnoult D, Stadler J, Posey AE, Hill RB, Blackstone C (2010). A lethal de novo mutation in the middle domain of the dynamin-related GTPase Drp1 impairs higher order assembly and mitochondrial division. J Biol Chem 285, 32494–32503.

Chappie JS, Acharya S, Leonard M, Schmid SL, Dyda F (2010). G domain dimerization controls dynamin's assembly-stimulated GTPase activity. Nature 465, 435–440.

Corpet F (1988). Multiple sequence alignment with hierarchical clustering. Nucleic Acids Res 16, 10881–10890.

Elgass KD, Smith EA, LeGros MA, Larabell CA, Ryan MT (2015). Analysis of ER-mitochondria contacts using correlative fluorescence microscopy and soft X-ray tomography of mammalian cells. J Cell Sci 128, 2795–2804.

Ferguson SM, De Camilli P (2012). Dynamin, a membrane-remodelling GTPase. Nat Rev Mol Cell Biol 13, 75–88.

Figueroa-Romero C, Iniguez-Lluhi JA, Stadler J, Chang CR, Arnoult D, Keller PJ, Hong Y, Blackstone C, Feldman EL (2009). SUMOylation of the mitochondrial fission protein Drp1 occurs at multiple nonconsensus sites within the B domain and is linked to its activity cycle. FASEB J 23, 3917–3927.

Francy CA, Alvarez FJ, Zhou L, Ramachandran R, Mears JA (2015). The mechanoenzymatic core of dynamin-related protein 1 comprises the minimal machinery required for membrane constriction. J Biol Chem 290, 11692–11703.

Frohlich C, Grabiger S, Schwefel D, Faelber K, Rosenbaum E, Mears J, Rocks O, Daumke O (2013). Structural insights into oligomerization and mitochondrial remodelling of dynamin 1-like protein. EMBO J 32, 1280–1292.

Gandre-Babbe S, van der Bliek AM (2008). The novel tail-anchored membrane protein Mff controls mitochondrial and peroxisomal fission in mammalian cells. Mol Biol Cell 19, 2402–2412.

Huang YJ, Acton TB, Montelione GT (2014). DisMeta: a meta server for construct design and optimization. Methods Mol Biol 1091, 3–16.

Ingerman E, Perkins EM, Marino M, Mears JA, McCaffery JM, Hinshaw JE, Nunnari J (2005). Dnm1 forms spirals that are structurally tailored to fit mitochondria. J Cell Biol 170, 1021–1027.

Ishihara N, Nomura M, Jofuku A, Kato H, Suzuki SO, Masuda K, Otera H, Nakanishi Y, Nonaka I, Goto Y, *et al.* (2009). Mitochondrial fission factor Drp1 is essential for embryonic development and synapse formation in mice. Nat Cell Biol 11, 958–966.

Kashatus DF, Lim KH, Brady DC, Pershing NL, Cox AD, Counter CM (2011). RALA and RALBP1 regulate mitochondrial fission at mitosis. Nat Cell Biol 13, 1108–1115.

Koirala S, Guo Q, Kalia R, Bui HT, Eckert DM, Frost A, Shaw JM (2013). Interchangeable adaptors regulate mitochondrial dynamin assembly for membrane scission. Proc Natl Acad Sci USA 110, E1342–E1351.

Lackner LL, Horner JS, Nunnari J (2009). Mechanistic analysis of a dynamin effector. Science 325, 874–877.

Loson OC, Liu R, Rome ME, Meng S, Kaiser JT, Shan SO, Chan DC (2014). The mitochondrial fission receptor MiD51 requires ADP as a cofactor. Structure 22, 367–377.

Loson OC, Song Z, Chen H, Chan DC (2013). Fis1, Mff, MiD49, and MiD51 mediate Drp1 recruitment in mitochondrial fission. Mol Biol Cell 24, 659–667.

Macdonald PJ, Stepanyants N, Mehrotra N, Mears JA, Qi X, Sesaki H, Ramachandran R (2014). A dimeric equilibrium intermediate nucleates Drp1 reassembly on mitochondrial membranes for fission. Mol Biol Cell 25, 1905–1915.

Mears JA, Lackner LL, Fang S, Ingerman E, Nunnari J, Hinshaw JE (2011). Conformational changes in Dnm1 support a contractile mechanism for mitochondrial fission. Nat Struct Mol Biol 18, 20–26.

Naylor K, Ingerman E, Okreglak V, Marino M, Hinshaw JE, Nunnari J (2006). Mdv1 interacts with assembled dnm1 to promote mitochondrial division. J Biol Chem 281, 2177–2183.

Otera H, Wang C, Cleland MM, Setoguchi K, Yokota S, Youle RJ, Mihara K (2010). Mff is an essential factor for mitochondrial recruitment of Drp1 during mitochondrial fission in mammalian cells. J Cell Biol 191, 1141–1158.

Palmer CS, Elgass KD, Parton RG, Osellame LD, Stojanovski D, Ryan MT (2013). Adaptor proteins MiD49 and MiD51 can act independently of Mff and Fis1 in Drp1 recruitment and are specific for mitochondrial fission. J Biol Chem 288, 27584–27593.

Palmer CS, Osellame LD, Laine D, Koutsopoulos OS, Frazier AE, Ryan MT (2011). MiD49 and MiD51, new components of the mitochondrial fission machinery. EMBO Rep 12, 565–573.

Reubold TF, Faelber K, Plattner N, Posor Y, Ketel K, Curth U, Schlegel J, Anand R, Manstein DJ, Noe F, *et al.* (2015). Crystal structure of the dynamin tetramer. Nature 525, 404–408.
Robert X, Gouet P (2014). Deciphering key features in protein structures with the new ENDscript server. Nucleic Acids Res 42, W320–W324.
Schmid SL, Frolov VA (2011). Dynamin: functional design of a membrane fission catalyst. Annu Rev Cell Dev Biol 27, 79–105.
Shen Q, Yamano K, Head BP, Kawajiri S, Cheung JT, Wang C, Cho JH, Hattori N, Youle RJ, van der Bliek AM (2014). Mutations in Fis1 disrupt orderly disposal of defective mitochondria. Mol Biol Cell 25, 145–159.
Smirnova E, Griparic L, Shurland DL, van der Bliek AM (2001). Dynamin-related protein Drp1 is required for mitochondrial division in mammalian cells. Mol Biol Cell 12, 2245–2256.
Stepanyants N, Macdonald PJ, Francy CA, Mears JA, Qi X, Ramachandran R (2015). Cardiolipin's propensity for phase transition and its reorganization by dynamin-related protein 1 form a basis for mitochondrial membrane fission. Mol Biol Cell 26, 3104–3116.
Strack S, Cribbs JT (2012). Allosteric modulation of Drp1 mechanoenzyme assembly and mitochondrial fission by the variable domain. J Biol Chem 287, 10990–11001.
Taguchi N, Ishihara N, Jofuku A, Oka T, Mihara K (2007). Mitotic phosphorylation of dynamin-related GTPase Drp1 participates in mitochondrial fission. J Biol Chem 282, 11521–11529.
Ugarte-Uribe B, Muller HM, Otsuki M, Nickel W, Garcia-Saez AJ (2014). Dynamin-related protein 1 (Drp1) promotes structural intermediates of membrane division. J Biol Chem 289, 30645–30656.
Van Criekinge W, Beyaert R (1999). Yeast two-hybrid: state of the art. Biol Proced Online 2, 1–38.
Wakabayashi J, Zhang Z, Wakabayashi N, Tamura Y, Fukaya M, Kensler TW, Iijima M, Sesaki H (2009). The dynamin-related GTPase Drp1 is required for embryonic and brain development in mice. J Cell Biol 186, 805–816.
Waterham HR, Koster J, van Roermund CW, Mooyer PA, Wanders RJ, Leonard JV (2007). A lethal defect of mitochondrial and peroxisomal fission. N Engl J Med 356, 1736–1741.
Wenger J, Klinglmayr E, Frohlich C, Eibl C, Gimeno A, Hessenberger M, Puehringer S, Daumke O, Goettig P (2013). Functional mapping of human dynamin-1-like GTPase domain based on x-ray structure analyses. PLoS One 8, e71835.
Westermann B (2010). Mitochondrial fusion and fission in cell life and death. Nat Rev Mol Cell Biol 11, 872–884.
Yamano K, Fogel AI, Wang C, van der Bliek AM, Youle RJ (2014). Mitochondrial Rab GAPs govern autophagosome biogenesis during mitophagy. Elife 3, e01612.
Yoon Y, Krueger EW, Oswald BJ, McNiven MA (2003). The mitochondrial protein hFis1 regulates mitochondrial fission in mammalian cells through an interaction with the dynamin-like protein DLP1. Mol Cell Biol 23, 5409–5420.
Youle RJ, van der Bliek AM (2012). Mitochondrial fission, fusion, and stress. Science 337, 1062–1065.
Zhao J, Liu T, Jin S, Wang X, Qu M, Uhlen P, Tomilin N, Shupliakov O, Lendahl U, Nister M (2011). Human MIEF1 recruits Drp1 to mitochondrial outer membranes and promotes mitochondrial fusion rather than fission. EMBO J 30, 2762–2778.
Zhu PP, Patterson A, Stadler J, Seeburg DP, Sheng M, Blackstone C (2004). Intra- and intermolecular domain interactions of the C-terminal GTPase effector domain of the multimeric dynamin-like GTPase Drp1. J Biol Chem 279, 35967–35974.

Supplemental Materials

Molecular Biology of the Cell

Liu et al.

Table S1. Drp1 mutants used in yeast two-hybrid screen

Mutant	Point mutations	Mutant	Point mutations
1	Q314A, Y315A, Q316A, S317A, L318A	22	E437A, Q440A, R441A
2	L319A, N320A, S321A, Y322A	23	Q444A, N448A, Y449A
3	G323A, P325A, V326A, D327A	24	H445A, C446A, S447A
4	S330A, T332A	25	Q452A, E453A, L455A, R456A
5	Q335A, L336A, T338A	26	K459A, H461A, D462A
6	K339A, T342A, N346A	27	D462A, V465A, E466A
7	T351S, A 352D, K353G, Y354Q	28	K474A, L476A, P477A, V478A
8	S358A, E359A, L360A	29	E481A, M482A, H484A, N485A
9	R365A, C367A, H371A	30	K497A, P499A
10	Y368A, E372A	31	D503A, A504R
11	G375A, T377A, S380A	32	E611A, R612A, K615A
12	R376A, E379A	33	L613A, S616A, Y617A
13	V381A, D382A, P383A, L384A	34	R622A, K623A, N624A, Q626A
14	G385D, G386E	35	D627A, S628A, K631A
15	I390A, T394A, R397A	36	H635A, F636A, N639A, H640A
16	N398A, T400A	37	K642A, D643A, T644A, Q646A
17	L406A, F407A, V408A, P409A	38	S647A, E648A, V650A, G651A
18	F413A, E414A, L415A, L416A	39	K655A, S656A, S657A, L658A, L659A
19	R419A, R423A, E425A	40	D660A, D661A, T664A
20	E426A, P427A, L429A, R430A	41	E667A, D668A, M669A
21	E433A, L434A, H436A	42	K674A, E675A, D678A

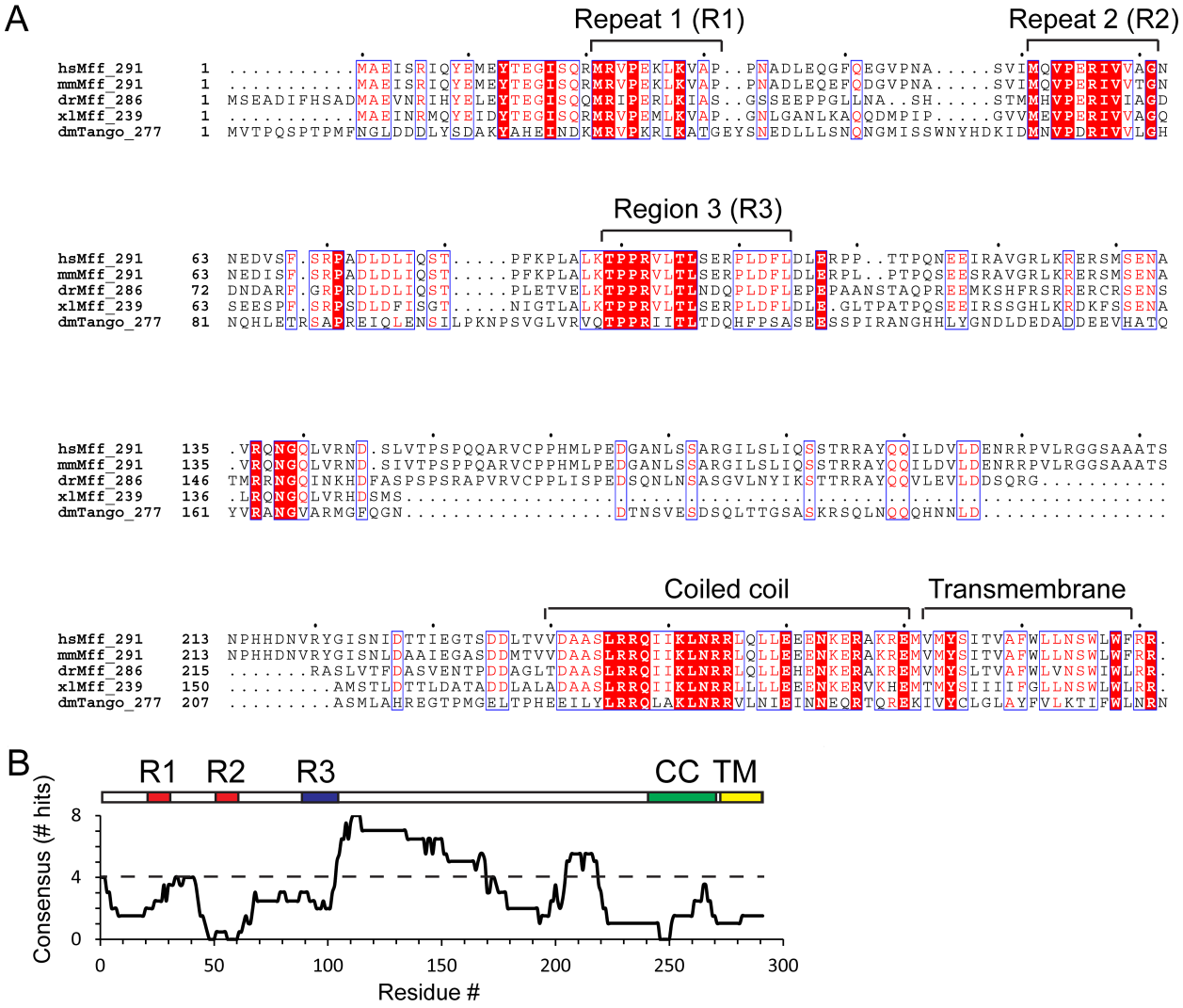

Figure S1. Mff sequence analysis.

(A) Multiple sequence alignment of Mff orthologs from human, mouse, fly, frog, and fish. Conserved residues are boxed in blue. Residues with 100% identity are highlighted in red with white text, and residues conserved in 70% of sequences are in red text. Notable regions included: Repeat 1 (R1) and Repeat 2 (R2) as previously identified (Gandre-Babbe and van der Bliek, 2008), an additional conserved region (R3), the coiled-coil domain (CC) and the transmembrane segment (TM). The Mff sequences used in this alignment are (RefSeq): *Homo sapiens* mitochondrial fission factor isoform b (NP_001263991.1), *Mus musculus* mitochondrial fission factor isoform 1, NP_083685.2, *Danio rerio* mitochondrial fission factor homolog A, (NP_001018402.2), *Xenopus laevis* mitochondrial fission factor homolog B, (NP_001085443.1), and *Drosophila melanogaster* transport and golgi organization 11, isoform A (NP_726111.1). Alignments were performed with MultAlin (Corpet, 1988) and formatted with ESPript (Robert and Gouet, 2014). (B) Disordered regions in Mff. DisMeta, the Disorder Prediction MetaServer (Huang *et al.*, 2014), was used to predict disordered regions in mouse Mff isoform 1. The consensus among 8 different predictors is plotted against each residue. A consensus above 50% of these predictors (dotted line) is indicative of disorder. The diagram of mouse Mff isoform 1 is aligned with the plot.

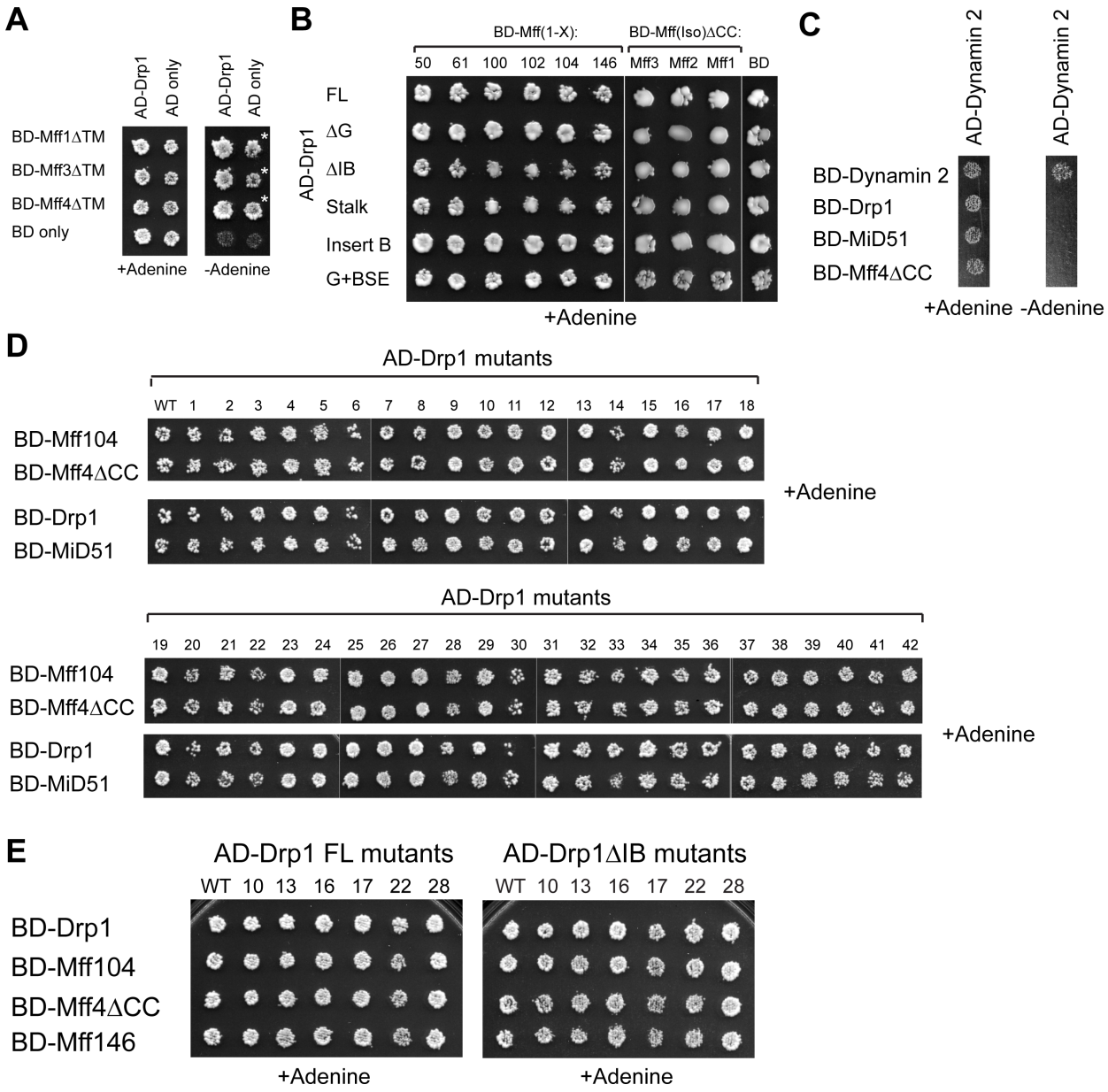

Figure S2. Yeast two-hybrid assay controls.

(A) Auto-activation of Mff lacking the transmembrane region. Mouse Mff isoforms 1, 3 and 4 with the transmembrane domain deleted (ΔTM) were expressed from the pGBDU vector as BD fusion proteins and tested against Drp1 expressed from the pGAD vector as AD fusion proteins. Growth on adenine-deficient plates, but not against AD or BD only, indicates an interaction. The growth of the Mff constructs against AD only on adenine-deficient plates (white asterisks) indicates auto-activation, making results with these constructs uninformative. (B) Diploid selection growths for the adenine-deficient plates in Figure 1E. (C) Lack of interaction between dynamin 2 and Mff. Mouse Dynamin 2, Drp1, MiD51, and Mff isoform 4 with the transmembrane domain deleted (Mff4ΔCC) were expressed as BD fusion proteins and tested against Dynamin 2 expressed as an AD fusion protein. Dynamin 2 interacted with itself, but did not interact with Drp1, MiD51, or Mff4ΔCC. (D) Diploid selection plates for the adenine-

deficient plates in Figure 3A. (E) Diploid selection plates for the adenine-deficient plates in Figure 3B.

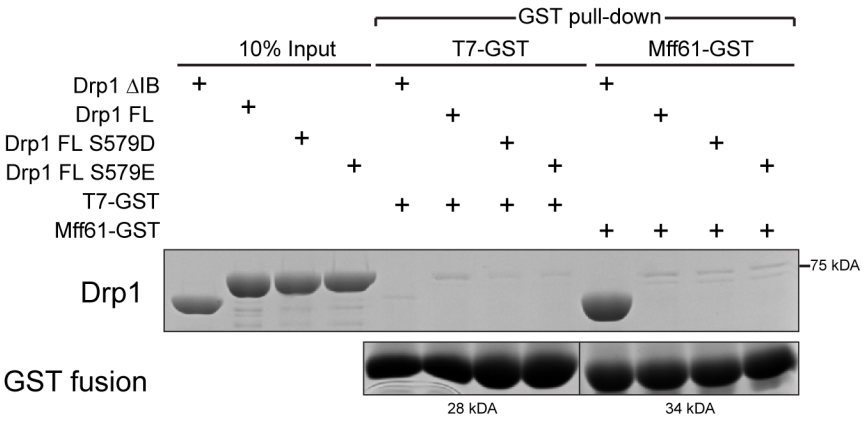

Figure S3. Phosphomimetic Drp1 does not interact with Mff61.
(A) GST pull-down assays for purified recombinant Drp1ΔIB, Drp1 (full-length), Drp1 S579D (full-length), and Drp1 S579E (full-length) versus purified recombinant Mff61-GST or T7-GST. The Coomassie-stained SDS-PAGE gel shows the input protein (lanes 1-4) and eluates from the pull-downs (lanes 5-12). In lanes 5-12, the bottom row shows the isolated GST fusion proteins. The top row depicts the co-immunoprecipitated proteins.